

NISTIR 6588

**FIFTEENTH MEETING OF THE UJNR
PANEL ON FIRE RESEARCH AND SAFETY
MARCH 1-7, 2000**

VOLUME 2

Sheilda L. Bryner, Editor



NIST

National Institute of Standards and Technology
Technology Administration, U.S. Department of Commerce

NISTIR 6588

**FIFTEENTH MEETING OF THE UJNR
PANEL ON FIRE RESEARCH AND SAFETY
MARCH 1-7, 2000**

VOLUME 2

Sheilda L. Bryner, Editor

November 2000



U. S. Department of Commerce

Norman Y. Mineta, Secretary

Technology Administration

Dr. Cheryl L. Shavers, Under Secretary of Commerce for Technology

National Institute of Standards and Technology

Raymond G. Kammer, Director

Flow Behavior under Sloped Ceiling

Osami Sugawa*, Takashi Hosozawa**, Naoto Nakamura*, Ayako Itoh*
and Yoshiyuki Matsubara***,

*Science Univ. of Tokyo, **Takenaka Co.,Ltd., ***Fire and Disaster Management Agency

Experimental study was carried out on the flow behavior which flows under the sloped ceiling. Temperature and flow velocity were measured to characterize the ceiling jet along the sloped ceiling surface. A diffusion gas burner was used as a model fire source giving 15-100kW, changing the slope angle of the ceiling adopting of 0, 30, 45, and 60 deg. Based on the experimental data, excess temperature and velocity along the sloped ceiling were modeled and which are usefully applicable to estimate the activation time of heat detector and sprinkler head mounted on the sloped ceiling. Excess temperature and flow velocity along the trajectory covering the flame to ceiling-jet regions were also modeled based on the Fr model.

Key Words: sloped ceiling, ceiling jet, temperature, velocity, Froude modeling

1. Introduction

Fire detectors and sprinkler system are important measures against a fire, especially in its early stage. Hot gas in the fire plume rise up and impinge on the ceiling. Heat detectors and sprinkler systems operate based on hot flow (excess temperature and flow velocity are main physical parameters which give the operating time based on RTI model) at the points where these system are monted. It is important and necessary to know the flow behavior under the ceiling to simulate the detecting and/or operating time for a fire protecting assessment. Alpert[1] had developed the modeling on gas temperature and velocity of the ceiling jet, and also Heskestad and Delichatsios[2][3] have proceeded the correlations between excess temperature and velocity. Alpert, Heskestad and Delichatsios, the leading researchers, have developed easy-to-use quantitative model on the gas temperature and velocity along a horizontal ceiling as the flow is produced from a steady burning of fire. These correlations are widely used in hazard analysis calculation. However, there is no easy-to-use model on the ceiling jet under the sloped ceiling such as a ceiling of stairway (part of underpass) and of a semicylindrical roof (quonset hut).

In this study, we carried out experimental study on the sloped ceiling jet using a semi-full scale

equipment. Based on the experimental data, the model was established which describes the excess temperature and flow velocity under the sloped ceiling. The model established here is applicable to predict the operation time of the heat detectors installed on the sloped ceiling.

2. Experimental Procedures

2.1 Unconfined Sloped Ceiling and Fire Source

We set up the sloped ceiling in an experiment room of 10m (W) x 8m (D) x 4m (H) which connects to the upper room having a ventilating system. The sloped ceiling is an unconfined square shape of 3.6m x 3.6m, as shown in Figure 1, and is composed of calcium silicate boards of 12mm

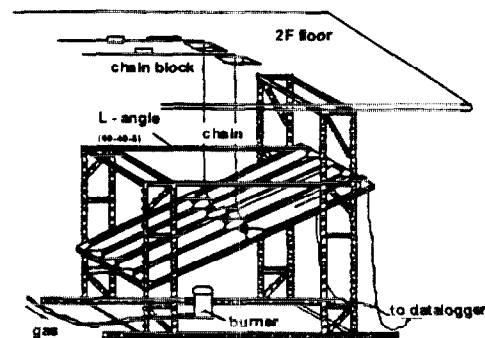


Figure 1. Experimental set-up of sloped ceiling

thick. A round sand gas burner, having 30cm high from the floor and diameter of 20cm ϕ , was set as a fire source under the cenetr line of the ceiling. Propane gas was supplied as a fuel.

Table1. Experimental Condition

angle (degree)	0						30					
HRR (kW)	15	20	30	45	80	100	15	20	30	45	80	100
ceiling height (m)	1.25	●	●	●	●	○	●	●	●	●	○	○
	1.5	●	●	●	●	○	●	●	●	●	○	○
	1.75	●	●	●	●	○	●	●	●	●	○	○
	2	●	●	●	●	○	●	●	●	●	○	○
	2.25	●	●	●	●	○	●	●	●	●	○	○
	2.5	●	●	●	●	○	●	●	●	●	○	○
angle (degree)	45						60					
HRR (kW)	15	20	30	45	80	100	15	20	30	45	80	100
ceiling height (m)	1.25	●	●	●	●	○	●	●	●	●	○	○
	1.5	●	●	●	●	○	●	●	●	●	○	○
	1.75	●	●	●	●	○	●	●	●	●	○	○
	2	●	●	●	●	○	●	●	●	●	○	○
	2.25	●	●	●	●	○	●	●	●	●	○	○
	2.5	●	●	●	●	○	●	●	●	●	○	○

2.2 Experimental Condition

Table1 shows the experimental conditions adopted in this study. The angle of sloped ceiling was adjusted to 0, 30, 45, and 60 degree, respectively. Heat release rate varied from 10kW to 100kW, and ceiling heights, 1.25m to 2.5m, were adopted systematically as Table1. The solid marks in Table 1 show the cases that the flame

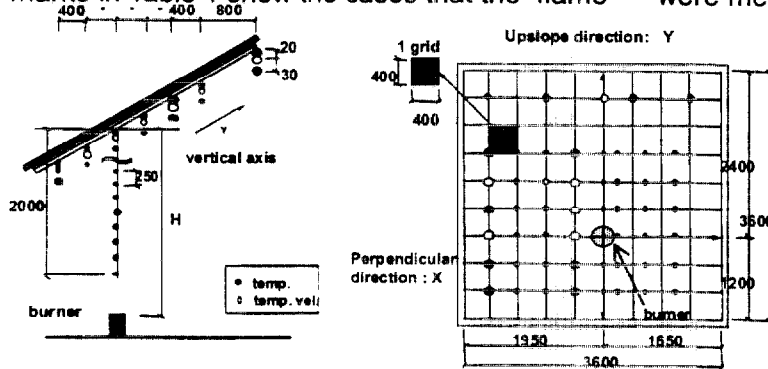


Figure 2. Measurement Points

did not cling to the ceiling, and the open marks show the ones that the flame or flame tip touched and extend along to the ceiling depending on heat release rate.

2.3 Measurements

The measurement were carried out on gas temperature and velocity under the sloped ceiling. Figure 2 shows the measurement points of the temperature and velocity. The temperatures

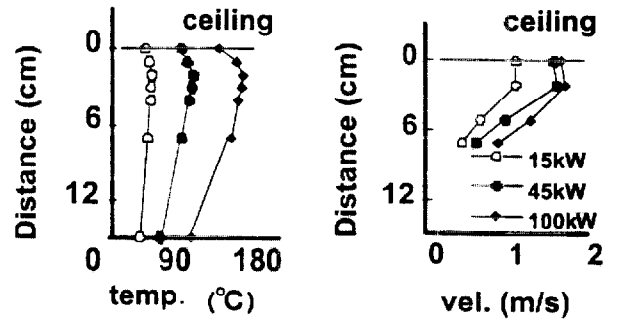


Figure 3.a Slope angle = 30deg

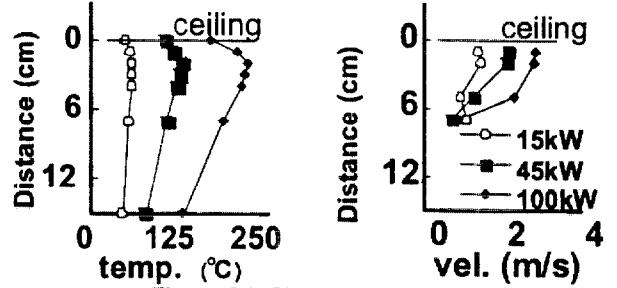


Figure 3.b Slope angle = 60 deg

Figure 3 Vertical distributions of excess temperature and flow velocity

were measured with K-type thermocouples, and the flow velocities were estimated based on the pressure difference obtained by bidirectional tubes. These data were recorded every 2 seconds during the steady condition.

3. Results and Discussion

3.1 Excess temperature and Velocity Distributions along Vertical Direction

Figure 3 shows the representative vertical distributions of the gas temperature and velocity at a distance of 1.2m apart from the cen-

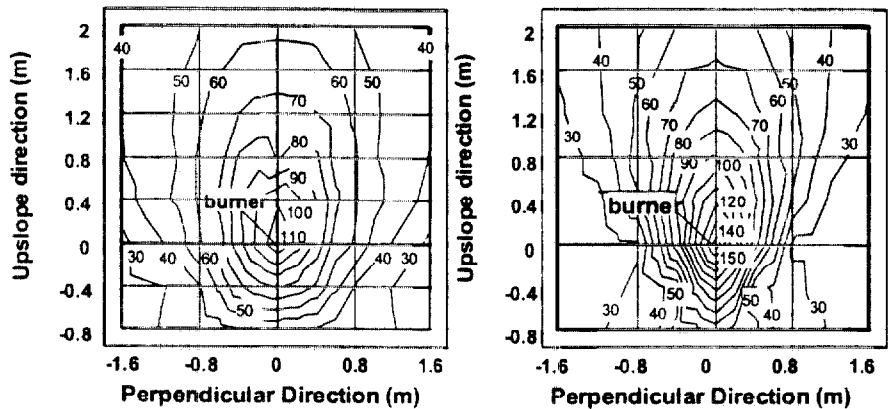


Figure 4.a Slope angle = 30 deg

Figure 4.b Slope angle = 60 deg

Figure 4 Representative excess temperature maps.

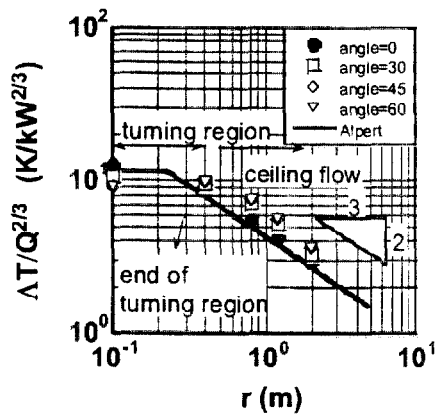


Figure 5.a Excess temperature

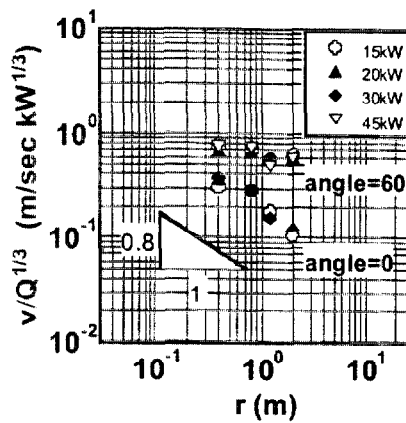


Figure 5.b Velocity along the ceiling surface

ter where the upward hot flow impinges on the ceiling and which show that the maximum temperature and velocity appeared about 2cm beneath the ceiling surface. In this study, therefore, the gas temperatures and velocities observed 2cm beneath the ceiling were adopted as representative values for description and analysis.

3.2 Temperature Distribution along the Upslope Direction

Figure 4.a and 4.b shows the representative temperature maps under the sloped ceiling surface. The temperature distribution of radial or elliptic-shape was observed for low sloped ceiling, and the distribution changed and expanded to round egg-shape as the ceiling angle is set steep. For downslope direction, radiation from flame tip gave apparent temperature rise resulting open end shape as Figure 4.

3.3 Characteristic Temperature and Flow Velocity along Upslope Direction

Figure 5.a shows the correlation between the excess temperature and the upslope pass distance, r , from the center. The turning region is formed around the center as was estimated based on ΔT and shown in Figure 5.a. However,

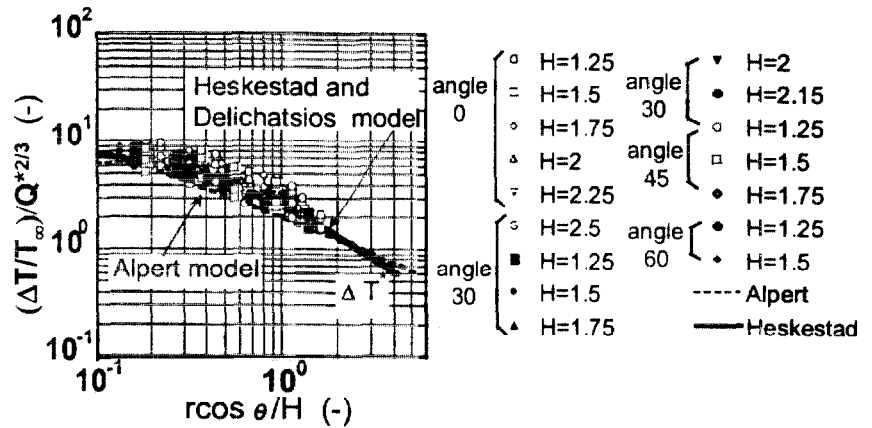


Figure 6. Dimensionless Temp. on Vertical Axis

it was very hard to distinguish clearly the boundary between impinging region and ceiling jet region based on the observation. In the turning region, the temperature decreasing rate is small, as shown in Figure 5.a, and then in the successive ceiling jet region the temperature decreased as $\Delta T \propto r^{-2/3}$ along the upslope trajectory.

As shown in Figure 5.b, the decreasing rate of velocity along the upslope ceiling showed remarkable change depending on the slope angle. Rough estimation on the decreasing rate for horizontal ceiling gave $v \propto r^{-1}$, and for steep sloped ceiling. As the slope angle set steeper and approached to the vertical situation, the decreasing mode of the flow velocity for upslope direction showed the same mode, $v \propto r^0$ as that observed from a line fire source.

3.4 Excess Temperature along Upslope Direction

Figure 6 shows the relation between dimensionless temperature rise and dimensionless path

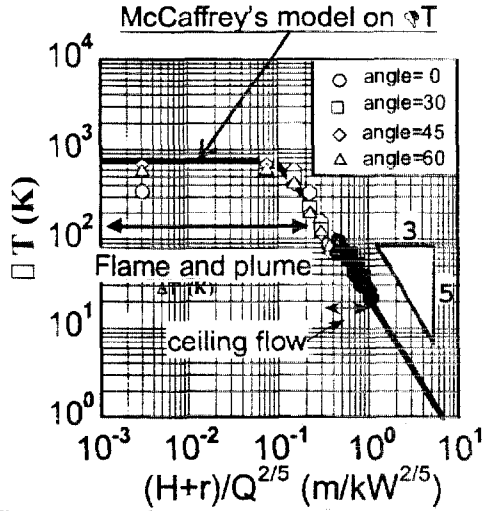


Figure 7.a Excess temperature distribution along the flow pass including flame, plume and ceiling jet regions. Thick line is given based on McCaffrey's model on flame and plume. $H=1.5m$ and $Q=20kW$

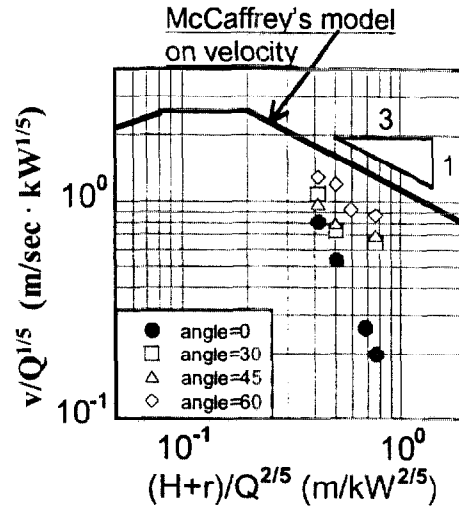


Figure 7.b Distribution of the flow velocity normalized by $Q^{1/5}$ along the trajectory including flame and ceiling jet regions. Thick line is given based on McCaffrey's model on flame and plume. $H=1.5m$ and $Q=20kW$

along the upslope trajectory. This figure is illustrated taking the same model with the Heskestad-Delcatsios' model. The established model on excess temperature model for upslope direction (Y-axis) are represented as followings:

$$\Delta T_{ver}^* = (0.41 + 0.2y/H)^{-4/3} \quad (\theta = 0) \quad (1.1 a)$$

$$\Delta T_{ver}^* = (0.41 + 0.4y \cos \theta / H)^{-4/3} \quad (0 < \theta \leq 90) \quad (1.1 b)$$

where $\Delta T^* = \left(\frac{\Delta T}{T_\infty} \right) / Q^{2/3}$ and $Q^* = Q / \rho_\infty c_p T_\infty \sqrt{g} H^{5/2}$

The coefficients of these formula are different

from the one of Heskestad-Delcatsios' model. This discrepancy may be given by the difference of the ceiling material used.

For the perpendicular direction against upslope direction (X-axis cf. Figure 2), the dimensionless temperature rise is also modeled as following:

$$\Delta T_{hor}^* = (a + 0.15x \sin \theta / H)^{-18} \quad (0 < \theta \leq 90) \quad (1.2)$$

where $a = (\Delta T_{ver}^*)^{-18}$

3.5 Correlation between Flow Velocity and Tem-

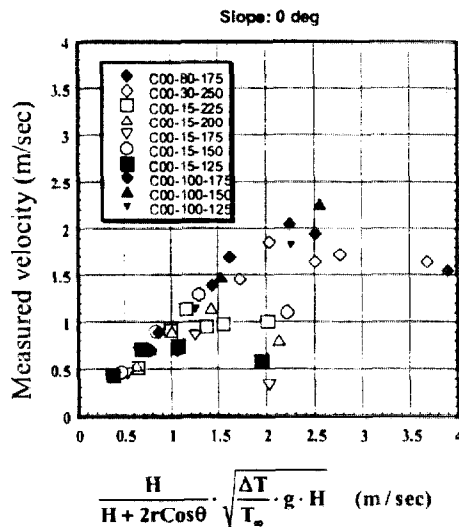


Figure 8 Correlation between measured velocity and temperature based velocity with location modification for slope angle of 0 deg.

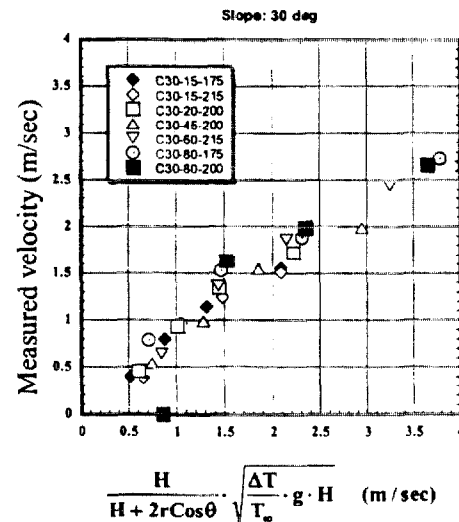


Figure 9 Correlation between measured velocity and temperature based velocity with location modification for slope angle of 30 deg.

perature based flow velocity of $\sqrt{(\Delta T / T_{\infty}) \cdot g \cdot H}$.

Flow velocity of the hot current resulted from buoyancy of flow produced by a fire source. This mechanism conserved not only in a flame/plume regions but also in ceiling jet region. Figure 7 shows the typical excess temperature distribution along the trajectory including in flame region and consecutive ceiling jet region. ΔT are plotted against the flow-pass which is total pass length including of height, H , and flow pass along the ceil-

ing r , i.e., $H+r$.

Figure 7 shows clearly that McCaffrey's model [4] of ΔT decreasing mode along the trajectory pass length,

$$\Delta T \propto (z/Q^{2/5})^{-5/3} \quad (3)$$

is applicable not only for flame but also for ceiling jet. However, Figure 7.b shows that McCaffrey's model on upward velocity for flame and plume is not acceptable for velocity for ceiling jet. These two figures imply the necessity of correction on the location which evaluate the flow-pass length including height and pass along the ceiling considering slope of the ceiling. We adopt the term of $H/(H+2r \cos \theta)$ to evaluate the location for temperature based velocity of $\sqrt{(\Delta T / T_{\infty}) \cdot g \cdot H}$ as is shown in Figure 8. Plots obtained in the turning region, where high excess temperatures are measured but direction of the flow is not established yet, show some gap from an apparent line which is formed by the gathering of plots obtained in the ceiling region consecutive to turning region. Figure 9 shows the same correlation as shown in Figure 8 illustrating the correlation between measured velocity and temperature based velocity with location modification of $H/(H+2r \cos \theta)$ for 30 deg sloped ceiling.

Modification term, $H/(H+2r \cos \theta)$, on location considering the ceiling slope works well to establish the conservation of Froude number.

Taking the same manner to the correlation between measured flow velocity, v , and temperature based velocity of $(H/(H+2r \cdot \cos \theta)) \cdot \sqrt{(\Delta T / T_{\infty}) g H}$ for other sloped ceiling changing the ceiling height. Figures 10 and 11 are illustrated for the slope angles of 45 deg and 60 deg, respectively. Both cases show also that the modification term on location including vertical height, H , and sloped flow pass, r , along the ceiling surface gave quite good performance to evaluate the flow velocity from the temperature based velocity. Based on the Figures 8 - 11, the measured flow velocity is modeled as

$$v = \alpha \cdot \frac{H}{H+2r \cdot \cos \theta} \cdot \sqrt{(\Delta T / T_{\infty}) \cdot g \cdot H} \quad (4)$$

where $\alpha \approx 3/4 \sim 7/8$, or Froude number is conserved along the trajectory in both regions of vertical flow (flame and plume) and ceiling jet flow independent of the slope angle.

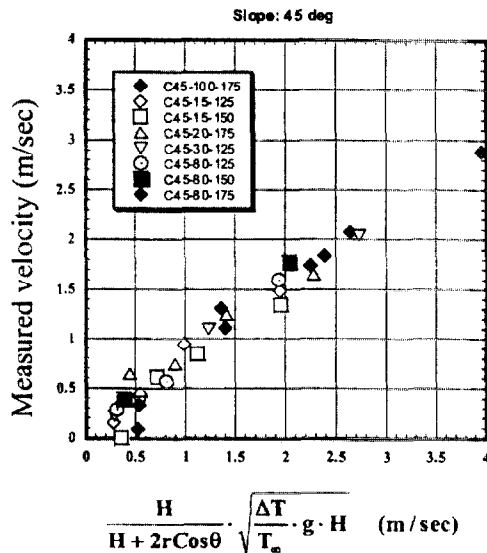


Figure 10 Correlation between measured velocity and temperature based velocity with location modification for slope angle of 45 deg.

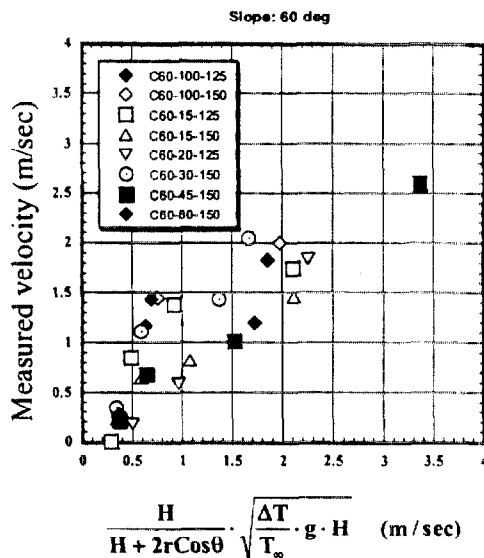


Figure 11 Correlation between measured velocity and temperature based velocity with location modification for slope angle of 60 deg.

$$Fr = \frac{v \cdot (H + 2r \cdot \cos\theta)}{\sqrt{\frac{\Delta T}{T_\infty} \cdot g \cdot H^{5/2}}} \approx \text{const} = \frac{3}{4} \sim \frac{7}{8} \quad (5)$$

As was shown in Figures 5.a and 7.a, and correlation obtained and presented in eq. (3), we can estimate the excess temperature, $\Delta T/T_\infty$, along the trajectory based on heat release rate, Q , ceiling height, H , slope angle, θ , and flow pass, r , along the ceilings. These physical values gave the flow velocity along the ceiling

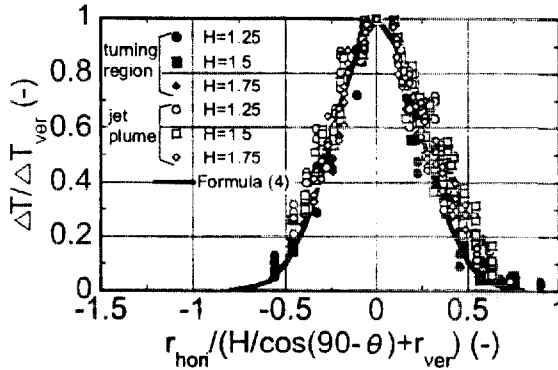


Figure 12.a Temperature Distribution in X Direction (slope angle=45°) $H=1.5\text{m}$, $Q=20\text{kW}$

using eqn. (4) so that we can estimate the detection time of heat detector and also operating time of sprinkler head.

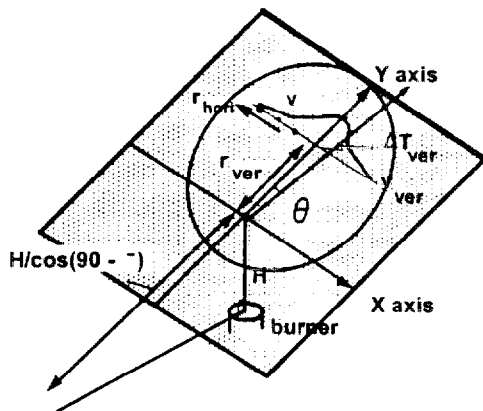


Figure 13 Layout of the coordinates for describe the distributions of excess temperature and flow velocity for perpendicular direction to upslope direction

3.6 Temperature and Flow Velocity for Perpendicular Direction -X Axis-

It is well known that upward gas flow velocity and excess temperature obtained in the plume region are simulated well by normal distributions (or Gaussian) respectively so that we could expected the same characteristic for the ceiling flow as it flows along the sloped ceiling surface. Figure 12.a shows the excess temperature distribution normalized by the maximum excess temperature which obtained along the trajectory of upslope direction (Y-axis). Figure 12.b shows the flow ve-

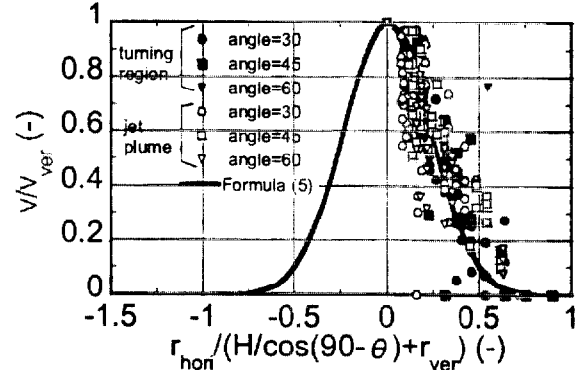


Figure 12.b Velocity Distribution in X Direction, $H=1.5\text{m}$, $Q=20\text{kW}$

locity distribution for perpendicular direction normalized by the maximum velocity obtained along the upslope trajectory (Y-axis). Both of these characteristics showed normal distributions as the original points is adopted as in Figure 13. followings:

$$\frac{\Delta T}{\Delta T_{\text{ver}}} = \exp(-\eta^2 \beta^2) \quad (6)$$

and

$$\frac{v}{v_{\text{ver}}} = \exp(-\eta^2 \beta^2) \quad (7)$$

where $\eta = r_{\text{hon}} / (H/\cos(90-\theta) + r_{\text{ver}})$ and $\beta = 3$

The temperature and velocity shown by equations (4) and (5) well simulated the experimental temperature and velocity.

4. Conclusion

Description model on excess temperature and velocity of the gas flow under the sloped ceiling were established considering the inclined angle.

The combination of location modification term of $H/(H+2r\cos\theta)$ and temperature based flow velocity, $\sqrt{(\Delta T/T_\infty) \cdot g \cdot H}$, gave conservation of Froude number for ceiling jet except turning region independent of slope angle. This correlation is excellent tool to predict the response time of the fire detectors (heat detector) and operation time of sprinkler which are mounted on the ceiling with and without slope angle.

McCaffery's model on excess temperature is applicable not only for flame and plume regions (vertical flow part) but also for the ceiling jet flow independent of the slope. This implies that there is no necessary to change the models to estimate excess temperature along the trajectory, i.e. vertical flow part (flame, intermittent flame and plume) by McCaffery's model and ceiling jet (horizontal ceiling) by Alpert's model.

Nomenclature

c_p	:heat capacity at constant pressure (kJ/kgK)
Fr^*	:Froude number (-)
g	:gravitational acceleration (m/s ²)
H	:ceiling height above fire source (m)
Q	:heat release rate (kW)
r	:distance from center along ceiling surface (m)
T	:gas temperature (K)
ΔT	:excess temperature (K)
V	:gas flow velocity (m/s)
β	:rate of expansion (-)
	:half width ratio of temperature to velocity (-)
θ	:slope angle of ceiling (°)
ρ_∞	:air density (kg/m ³)

Subscripts

<i>ver</i>	:along vertical axis (Y-axis)
<i>hor</i>	:along horizontal axis (X-axis)
∞	:ambient, outside ceiling jet or plume flows

Superscripts

\cdot	:dimensionless quantity
---------	-------------------------

References

- [1] R.L.Alpert : Calculation of Response Time of Ceiling-Mounted Fire Detectors, Fire Technology, Vol.8,181-195,1972
- [2] G. Heskestad and Michael A.Delichatsios : The Ini

tial Convective Flow in Fire, 17th International Symposium on Combustion, Combustion Institute, Pittsburgh (1978)

- [3] David D.Evans :Ceiling Jet Flows, The SFPE Handbook of FIRE PROTECTION ENGINEERING, Ver.1, 1963
- [4] McCaffery B.J. :Purely Buoyant Diffusion Flames, NBSIR79-1910, 1979